NEUROSCIENCE

Overwriting an instinct: Visual cortex instructs learning to suppress fear responses

Sara Mederos[1]*, Patty Blakely[1], Nicole Vissers[1], Claudia Clopath[1,2], Sonja B. Hofer[1]*

Fast instinctive responses to environmental stimuli can be crucial for survival but are not always optimal. Animals can adapt their behavior and suppress instinctive reactions, but the neural pathways mediating such ethologically relevant forms of learning remain unclear. We found that posterolateral higher visual areas (plHVAs) are crucial for learning to suppress escapes from innate visual threats through a top-down pathway to the ventrolateral geniculate nucleus (vLGN). plHVAs are no longer necessary after learning; instead, the learned behavior relies on plasticity within vLGN populations that exert inhibitory control over escape responses. vLGN neurons receiving input from plHVAs enhance their responses to visual threat stimuli during learning through endocannabinoid-mediated long-term suppression of their inhibitory inputs. We thus reveal the detailed circuit, cellular, and synaptic mechanisms underlying experience-dependent suppression of fear responses.

Instinctive behaviors are automatic responses to specific environmental challenges that have evolved to furnish animals with a repertoire of behaviors vital for survival and reproductive success. These behaviors allow animals to quickly detect and respond to potential dangers or opportunities in their environment without the need for prior learning or experience (*1*, *2*) and are usually implemented by brainstem pathways independent of neural processes in the forebrain (*3*–*5*). However, to ensure continuing success in changing environments, it is also important to be able to suppress instinctive reactions if they are no longer appropriate or advantageous (*6*–*9*). Many animals can modify instinctive behaviors based on experience or changing circumstances (*5*, *7*, *10*–*14*). This behavioral flexibility allows them to fine-tune responses to their specific environment to conserve resources, avoid unnecessary risks, or capitalize on new opportunities. The neural basis of this ethologically highly relevant form of learning, the overwriting of instinctive reactions, is still unclear.

Fear responses to visual threats, such as escape from an approaching aerial predator, are examples of instinctive reactions particularly crucial for survival (*1*, *3*, *4*, *15*, *16*). Escapes from overhead looming stimuli mimicking aerial predators are mediated by neural circuits involving the medial superior colliculus and the periaqueductal gray (*3*, *17*–*19*). This visuo-motor pathway in the brainstem autonomously drives escape responses independently of the forebrain (*3*, *20*). However, animals can suppress these fear responses as they learn that a perceived visual threat proves harmless (*5*, *7*, *10*, *11*, *14*, *21*), and this form of adaptive behavior may involve neocortical circuits. Sensory circuits in the neocortex can modulate different forms of instinctive or reflexive reactions to sensory stimuli (*12*, *22*–*24*). Higher visual areas (HVAs) in rodents integrate both visual and diverse behavioral and task-related variables and have been linked to numerous functions that go beyond basic visual processing (*25*–*29*). HVAs posterolateral to the primary visual cortex (V1) contribute to learning and execution of various learned visually guided behaviors. These areas, including the postrhinal, lateromedial, posteriomedial, and laterointermediate cortices, which we will collectively refer to as posterolateral HVAs (plHVAs), are also important for encoding visual and spatial context, are modified by prior experience, and have been shown to adaptively modulate innate behaviors (*22*, *25*, *26*, *30*–*33*). plHVAs thus may provide suitable candidate regions for implementing experience-dependent control over visually driven instincts through their extensive cortico-fugal projections. One pathway that provides visual cortical areas with a route to exert strong inhibitory control over brainstem processing and, thus, over behavioral output, is the dense projection to the ventrolateral geniculate nucleus (vLGN) in the prethalamus (*11*, *34*–*36*). Prethalamic areas, including the vLGN and the adjacent zona incerta, are part of the diencephalon, consist mainly of GABAergic neurons, and act as inhibitory control hubs of diverse instinctive behaviors (*35*, *37*). The vLGN, in particular, receives visual input from the retina and has powerful control over fear responses to visual threat (*11*, *35*, *36*).

Higher visual cortex is crucial for learning to suppress instinctive fear responses

Escape behavior evoked by a looming (i.e., dark overhead expanding) stimulus is a well-established protocol for assessing instinctive fear responses (*3*, *15*). When naïve mice are presented with this visual stimulus, they consistently escape to a shelter provided at the other end of an elongated arena (Movie 1). However, mice can adapt their behavior and suppress this fear response if they learn that the potential threat stimulus does not result in negative consequences (*10*, *11*). But, if animals are given the opportunity to seek shelter, then they often keep escaping to high-contrast looming stimuli for many stimulus repetitions and several behavioral sessions (fig. S1, A and B). We therefore adapted a protocol developed by Lenzi and colleagues (*10*) in which we prevented access to the shelter with a dividing barrier and presented looming stimuli with increasing contrast (acquisition phase, Fig. 1A and Movie 2). We then removed the barrier and assessed the likelihood of mice to escape from high-contrast looming stimuli (probe phase, Fig. 1A). Control mice showed strongly decreased fear responses after this learning protocol, and only rarely escaped from the looming stimulus (Fig. 1B; Movie 3; and fig. S2A).

To test whether neural activity in plHVAs is important for this learned suppression of escape responses, we used transgenic mice expressing channelrhodopsin-2 (ChR2) in GABAergic neurons and implanted optical fibers to silence neural activity bilaterally in plHVAs with blue light (*38*). Silencing plHVAs while presenting looming stimuli in naïve mice had no effect on the animals' probability to escape or other behavioral measures (fig. S2C), consistent with

Movie 1. Escape behavior in response to looming stimulus presentation in a naive example mouse.

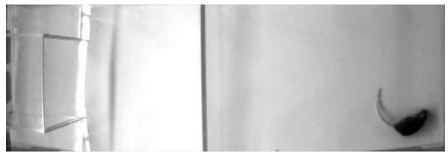

Movie 2. Looming stimulus presentation in an example mouse during the learning protocol with the barrier.

Movie 3. Lack of escape to looming stimulus presentation in an example mouse after the learning protocol.

[1]Sainsbury Wellcome Centre, University College London, London, UK. [2]Bioengineering Department, Imperial College London, London, UK.
*Corresponding author. Email: smederos.cr@gmail.com (S.M.); s.hofer@ucl.ac.uk (S.B.H.)

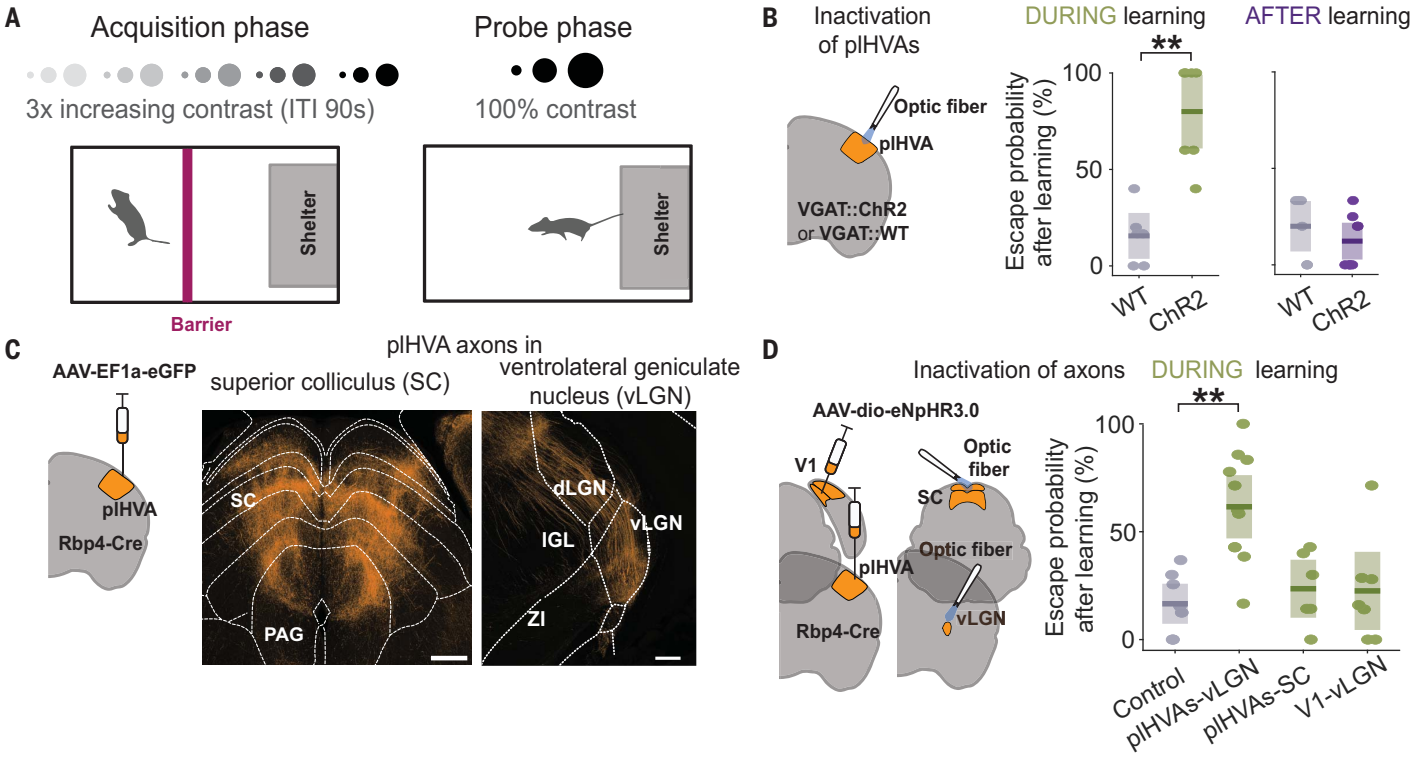

Fig. 1. plHVAs instruct learning through corticofugal projections to the vLGN. (**A**) Schematic of the task and stimulus protocols. Acquisition phase: A barrier is used to prevent escape to a shelter while looming stimuli with increasing contrast are shown sequentially. Probe phase: The barrier is removed and 6 to 10 100%-contrast looming stimuli are shown. ITI, intertrial interval. (**B**) (Left) Experimental approach. (Middle) Boxplot (showing median and interquartile range) of escape probability after learning with (green) and without (gray) silencing of plHVAs during learning. Dots show individual animals. $P = 0.003$, Kruskal-Wallis test; $n = 6$ [wildtype (WT) control] and 7 mice (ChR2, green). (Right) Same as middle, but plHVAs are silenced only after learning. $P = 0.222$, Kruskal-Wallis test; $n = 6$ (WT control) and 8 mice (ChR2, purple). (**C**) (Left) Schematic of tracer injection in plHVAs. (Right) Labeled plHVA axons in different target areas. Scale bars, 500 (left) and 250 μm (right). PAG, periaqueductal gray; SC, superior colliculus; IGL, intergeniculate leaflet; dLGN, dorsal geniculate nucleus; ZI, zona incerta; eGFP, enhanced green fluorescent protein. (**D**) (Left) Experimental design. (Right) Boxplots of escape probabilities after learning in control animals and when plHVA axons in vLGN (plHVA-vLGN) or SC (plHVA-SC) are silenced, or when V1 axons in vLGN are silenced during learning (V1-vLGN). Dots represent individual animals. plHVA-vLGN versus control, $P = 0.003$; plHVA-SC versus control, $P = 0.856$; V1-vLGN versus control, $P = 0.973$; Kruskal-Wallis test; $n = 8$, 11, 6, and 7 mice, respectively. $^{**}P < 0.01$.

previous results showing that visual cortex has little influence on the instinctive escape response to visual threats (*3*). However, when plHVAs were silenced during the learning protocol (during all stimulus presentations in the acquisition phase), mice failed to learn and still showed high escape probabilities to looming stimuli in the probe phase (Fig. 1B, center). We repeated these experiments with a long learning protocol with access to the shelter, in which mice eventually ceased to escape after presentation of high-contrast looming stimuli over several days (fig. S1). Silencing plHVAs with muscimol had little effect on instinctive escape behavior in naïve mice but, when applied throughout the learning protocol, prevented mice from learning to suppress escape responses (fig. S1, A to C), corroborating that plHVAs are necessary for learning to suppress escape responses independent of the experimental protocol. By contrast, optogenetic silencing of plHVAs only after mice had learnt had no effect on the learnt behavior, as mice still suppressed escape responses when plHVAs were silenced (Fig. 1B, right, and fig. S2B).

plHVA input to vLGN mediates learning to suppress fear responses

We next aimed to identify the specific pathways through which plHVAs mediate learnt suppression of fear responses. Anterograde axon labeling from layer 5 (L5) neurons in plHVAs using Rbp4-Cre mice showed dense projections in several subcortical regions, including the medial and deep layers of the superior colliculus (SC), previously shown to be crucial for generating escape responses to looming stimuli (*3*, *17*). Another clear target of plHVA projections was the vLGN (Fig. 1C), an inhibitory prethalamic area that has strong control over fear behavior and that, when activated, can fully block escape responses by inhibiting SC activity (*11*, *35*, *36*). To test the relevance of these two plHVA pathways for learning, we optogenetically silenced plHVA axonal projections selectively in either SC or vLGN by optical stimulation of halorhodopsin eNpHR3.0–expressing plHVA axons during the acquisition phase of the learning protocol (Fig. 1, A and D). Silencing plHVA projections to vLGN prevented learning, as mice continued to escape to the looming stimulus afterwards (Fig. 1D). By contrast, silencing plHVA projections to SC had no effect on learning (Fig. 1D). Moreover, silencing projections from V1 to vLGN also did not affect learning, showing that it is specifically projections from plHVAs to vLGN that are necessary for mice to learn to suppress escape responses (Fig. 1D and fig. S3, A to D). We corroborated the necessity of the plHVA-to-vLGN pathway for learning with a chemogenetic approach by which we targeted the inhibitory designer receptor hM4Di selectively to plHVA L5 neurons in Rbp4-cre mice and applied the agonist Clozapine *N*-oxide locally in vLGN or SC (fig. S3, E and F). Chemogenetic silencing of projections from plHVA to vLGN but not to SC also impeded learning.

plHVA-innervated vLGN cells are necessary and sufficient for suppression of escape responses

The experience of looming stimuli during the learning protocol likely induces lasting changes in neural circuits, i.e., a memory of this prior experience, leading to the adapted behavioral response to the visual threat stimulus. Our data show that, although plHVAs are required

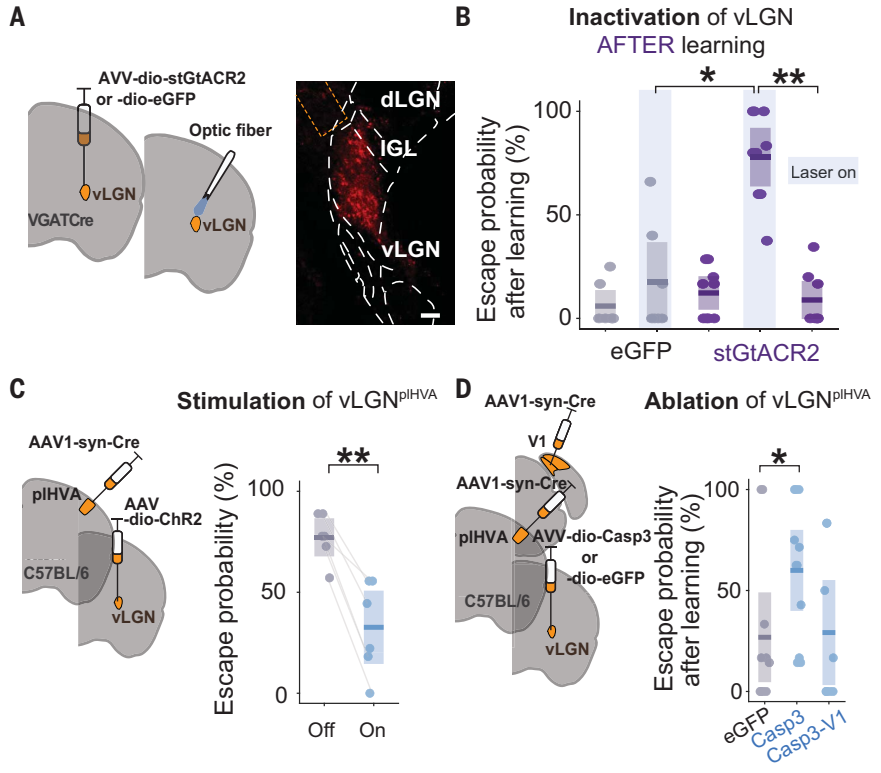

Fig. 2. vLGN cells receiving plHVA input are necessary for learning. (**A**) (Left) Experimental approach for acute inhibition of vLGN. (Right) Example image of vLGN neurons expressing stGtACR2. Scale bar, 150 μm. (**B**) Boxplot (showing median and interquartile range) comparing postlearning escape probabilities to 6 to 10 high-contrast looming stimuli for control mice expressing eGFP in vLGN with and without laser (gray, n = 7 mice, P = 0.954, Kruskal-Wallis test) and mice with stGtACR2 expression in GABAergic vLGN neurons without laser, with laser, and, subsequently, without laser again [purple, n = 9 mice, without before versus with laser: P = 0.0057 repeated-measures analysis of variance (ANOVA); with laser versus without laser after: P = 0.0020, repeated-measures ANOVA; laser eGFP versus laser stGtACR2: P = 0.005, Kruskal-Wallis test]. (**C**) (Left) Experimental approach for activating vLGN cells receiving input from plHVAs (vLGN^{plHVA} neurons). (Right) Boxplot of escape probabilities to 100%-contrast looming stimuli of naive mice without (off, gray) or with activation of plHVA-innervated vLGN neurons expressing ChR2 (on, blue; P = 0.004, paired t test, n = 6 mice). (**D**) (Left) Experimental approach for specifically lesioning plHVA- or V1-innervated vLGN cells. (Right) Boxplot of postlearning escape probabilities of control mice (gray, n = 7 mice) and mice with plHVA-innervated vLGN cells ablated before learning (blue, n = 11 mice, P = 0.039, Wilcoxon rank sum test) or V1-innervated vLGN cells ablated before learning (blue, n = 7 mice, P = 0.886, Wilcoxon rank sum test). Dots represent individual animals. *P < 0.05; **P < 0.01.

for learning to suppress fear responses, they are no longer necessary after learning. This indicates that the learning-induced memory is stored in neural circuits downstream of plHVAs. Because activation of vLGN by plHVA projections is necessary for learning, vLGN is one potential substrate for memory formation. We therefore set out to test this hypothesis. First, we examined if activity in vLGN is required for the adapted behavioral response, i.e., the suppression of escape to looming stimuli after learning. We expressed Cre-dependent stGtACR2 in vLGN of VGAT-Cre mice through AAV injections to optogenetically silence inhibitory cells, which constitute the large majority of vLGN neurons (*11*, *34*, *35*). When we silenced vLGN during stimulus presentation after learning (in the probe phase), mice resumed escaping from looming stimuli (Fig. 2A, B). This suggests that, unlike plHVAs, vLGN is necessary for the learned behavioral response. Mice immediately reverted to the learned behavior of suppressing escape responses when optogenetic manipulation was switched off, indicating that transient inhibition of vLGN neurons did not cause a sustained increase in a fear- or anxiety-related state (Fig. 2B).

However, silencing of vLGN could generally lower the threshold for threat-evoked escape responses independently of the plHVA-dependent learning process (*11*, *36*). To test the role of the plHVA-vLGN pathway in learned suppression of escape responses more specifically, we selectively targeted vLGN neurons receiving input from plHVAs by combining anterograde transfer of Cre recombinase from plHVAs to vLGN and Cre-dependent gene expression in vLGN (see materials and methods; fig. S4). vLGN neurons receiving input from plHVAs were GABAergic cells projecting to SC and other target areas (fig. S4). Expressing ChR2 specifically in these plHVA-innervated vLGN neurons and activating them during looming stimulus presentation suppressed mice's escape responses (Fig. 2C and movies S1 and S2), showing that increased activity in these neurons is sufficient to produce the learned behavior without prior experience of looming stimuli. Moreover, when we ablated plHVA-innervated vLGN neurons using Cre-dependent caspase expression (Fig. 2D, left), mice showed impaired learning with a higher likelihood to escape from looming stimuli than control mice after the learning protocol (Fig. 2D, right). By contrast, ablating V1-innervated vLGN cells had no effect on learning, even though these neurons constitute a larger fraction of vLGN cells (Fig. 2D and fig. S4, G and H).

plHVA-innervated vLGN neurons increase their looming responses over learning

To determine how neural activity in vLGN changes during learning, we performed electrophysiological single-unit recordings during presentation of high-contrast looming stimuli. We recorded over many stimulus presentations until animals learned not to escape (long learning protocol; see also fig. S1) and tracked responses of the same neurons over learning by using chronically implanted silicon probes in vLGN (Fig. 3A, fig. S5, and materials and methods). We selected cells responsive to the looming stimulus within 0 to 300 ms after stimulus onset (before learning, after learning, or both). Restricting the analysis to this early time window allowed us to isolate visual signals and minimize the influence of motor-related activity because the average escape latency of mice was 1.73 ± 0.08 s (mean ± SD), and we excluded the few trials in which mice initiated an escape earlier than 300 ms after stimulus onset (fig. S6, D and E). Moreover, mice exhibited freezing before escapes in a subset of trials, and neural activity was not different in escape versus freezing trials, indicating that these early stimulus responses in vLGN were not affected by the animals' behavior (fig. S6, A to C). vLGN neurons exhibited diverse responses to looming stimuli, and many neurons changed their activity during learning. To capture such changes, we divided neurons depending on whether they significantly increased their firing rate, decreased their firing rate, or showed no change in looming stimulus response over learning (Fig. 3, B to D).

In a subset of animals, we expressed ChR2 in L5 neurons of plHVAs in Rbp4-Cre mice to combine electrophysiological recordings of vLGN cells with optogenetic activation of plHVA axons in vLGN. This allowed us to identify vLGN neurons excited by plHVAs (positively modulated), inhibited (negatively modulated), or not affected by plHVA axon activation, and these groups of neurons showed differences in their electrophysiological properties and in how their looming stimulus responses changed over learning

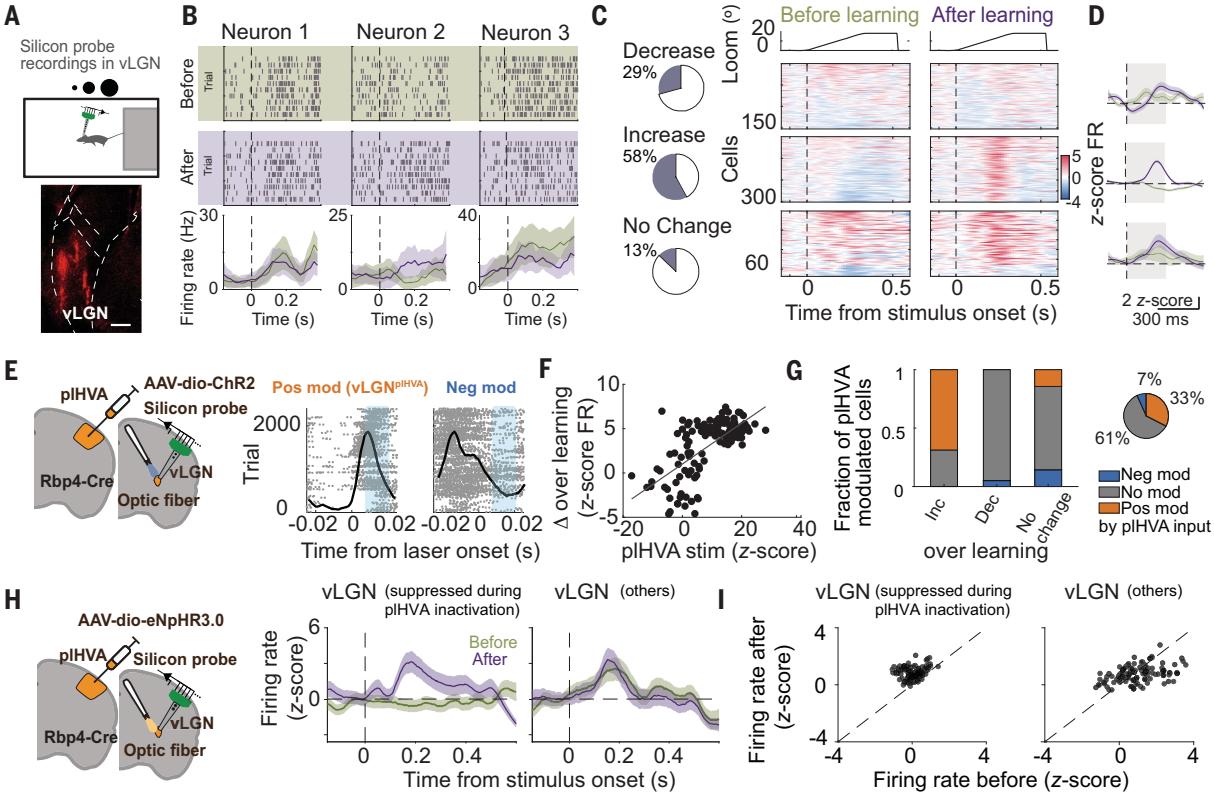

Fig. 3. plHVA-innervated vLGN neurons increase responses to looming stimuli during learning. (**A**) (Top) Experimental approach: Chronic electrophysiological recordings in vLGN while freely-moving animals are exposed to high-contrast looming stimuli until they learn to suppress escape responses. (Bottom) Example image with probe shank locations. Scale bar, 200 μm. (**B**) Looming stimulus responses of three vLGN example cells before and after learning. (**C**) (Left) Pie charts of fraction of vLGN neurons with increased and decreased responses or no change in response strength over learning in a time window of 0 to 300 ms after stimulus onset. (Right) *Z*-scored spike rate responses aligned to looming stimulus onset of all isolated units classified as looming-stimulus responsive neurons (from n = 9 mice) before or after learning, allocated according to their response change over learning. (**D**) Mean peristimulus histograms (PSTHs) of looming responses before and after learning of the three groups of vLGN neurons in (C). The dashed lines show stimulus onset, and the shaded areas denotes time window used for analysis [n = 152, 301, and 67 cells (top to bottom) from 9 mice]. (**E**) (Left) Experimental design. (Right) Spike responses to optogenetic stimulation of plHVA axons and PSTHs for example vLGN neurons. (**F**) Change (Δ) in looming stimulus response magnitude over learning of individual vLGN neurons as a function of their response magnitude to plHVA stimulation (correlation coefficient r = 0.680, P < 0.0001, Pearson correlation; n = 131 cells from 5 mice). FR, firing rate. (**G**) (Left) Fraction of negatively modulated (neg mod), positively modulated (pos mod), and nonmodulated neurons (no mod) during stimulation of plHVAs for vLGN neurons that increase, decrease, or show no change in response to looming stimuli over learning. (Right) Pie chart shows the fraction of units exhibiting modulation by plHVA activation out of all recorded neurons (n = 175, 302, and 36 cells from 5 mice). (**H**) (Left) Experimental design. (Right) Mean PSTHs in response to looming stimuli for neurons suppressed during plHVA silencing (left) and other vLGN neurons (right). [n = 108 (left) and 281 cells (right) from 4 mice]. Green, before learning; purple, after learning. (**I**) Scatterplots of looming stimulus response strength before and after learning (0 to 300 ms after stimulus onset) for individual vLGN neurons divided as in (H) (suppressed during plHVA silencing, P < 0.0001; other vLGN neurons, P = 0.0521; Wilcoxon signed-rank tests).

(Fig. 3, E to G, and fig. S7). The large majority of vLGN neurons excited by plHVAs increased their responses to looming stimuli during learning (Fig. 3, E to G), indicating a crucial role for plHVA inputs in shaping vLGN responses to looming stimuli over learning. To corroborate these findings and test whether plHVA inputs contribute to looming responses of vLGN neurons, we performed another set of experiments in which we optogenetically inactivated plHVAs inputs to vLGN using eNpHR3.0 during a subset of interleaved looming stimuli trials while recording from vLGN neurons. We identified vLGN neurons receiving excitatory input from plHVAs as those that were significantly suppressed during plHVA inactivation (fig. S8, A to C). These vLGN neurons again showed on average a clear increase in looming stimulus responses over learning (Fig. 3, H and I), even when plHVA input was removed (fig. S8). By contrast, the remaining vLGN population showed on average no response change over learning (Fig. 3, H and I). The time course of looming response increase in vLGN neurons was tightly correlated with the time course of behavioral changes over the session: mice that showed earlier increases in vLGN looming responses also learned faster (fig. S7F). Both plHVA activation and inactivation experiments show that it is predominantly those vLGN neurons receiving excitatory input from plHVAs that increase their firing responses to looming stimuli over learning. Notably, as demonstrated above, these vLGN neurons are necessary for learning to suppress escape responses, and increases in their neural looming response cause suppression of escape (Fig. 2, C and D).

Decreased inhibition onto plHVA-innervated vLGN neurons through endocannabinoid-mediated plasticity

Next, we set out to explore the potential cellular and synaptic mechanisms of this learning-induced change in vLGN activity. To determine whether functional interactions between different groups of vLGN neurons change during learning, we calculated pairwise cross-correlation functions of the spike trains of all simultaneously

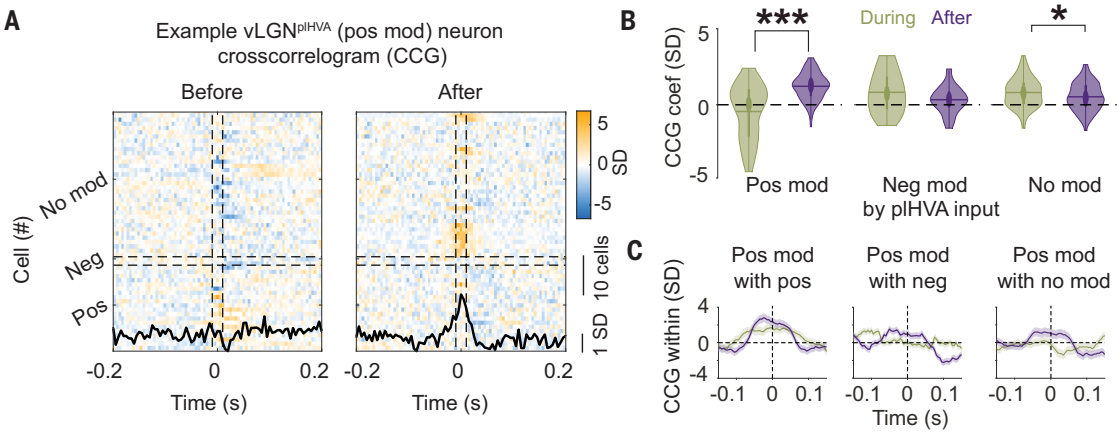

Fig. 4. Inhibitory influence on plHVA-innervated vLGN neurons may be decreased during learning. (**A**) Cross-correlograms (CCGs) of temporal spiking relationships (excluding periods of looming stimulus presentation) before and after learning between an example vLGN neuron positively modulated by plHVA activation (vLGN^{plHVA}) and all other simultaneously recorded units (each row in the heatmap shows a CCG of one neuron with one other unit: the spiking variation of the example neuron conditioned on the spiking of one other neuron at time 0). The black line represents the average of all CCGs in the plot. (**B**) Average CCG spiking variation around lag 0 (−1 to +4 ms) and distribution for all vLGN neurons positively, negatively, or not modulated during plHVA optogenetic activation with the rest of the vLGN population before (green) and after (purple) learning [before versus after learning: pos mod, $P < 0.001$; neg mod, $P = 0.785$; no mod, $P = 0.011$; Kruskal-Wallis test; $n = 121$, 29, and 249 cells (from left to right) from 5 mice]. Coef, coefficient. (**C**) Average spike CCG for all vLGN neurons positively modulated by plHVA stimulation with other neurons from the three groups before (green) and after (purple) learning. *$P < 0.05$; ***$P < 0.001$.

recorded vLGN neurons. Neurons that were positively modulated by plHVA activation again stood out in that many of them had negative spike time correlations with the rest of the vLGN network, especially with the neurons not affected by plHVA activation (Fig. 4, A to C, and fig. S9, A and B). For many of these cell pairs, the troughs in the cross correlogram were biased toward positive time lags (fig. S9C), suggesting that neurons that receive plHVA input may be inhibited by the local vLGN network before learning. This is consistent with the observation that these vLGN neurons are inhibited by looming stimuli before learning, particularly when excitatory plHVA input is removed (fig. S8D). Spike timing relationships, specifically between vLGN neurons positively modulated by plHVA activation and the rest of the network, changed with learning, such that these neurons showed positive correlations with the remaining vLGN neurons after learning, suggesting a release from inhibition over learning (Fig. 4, A to C, and fig. S8).

A potentially related form of synaptic plasticity, long-term depression of inhibition (iLTD), has been described in multiple brain areas in vitro and is dependent on endocannabinoid (eCB) signaling (*39*–*43*). Heterosynaptic iLTD can be triggered by activation of group I metabotropic glutamate receptors (mGluR1 or mGluR5) in postsynaptic neurons (*41*, *42*, *44*). This causes release of eCBs, which act as retrograde messengers, activating eCB receptors (CB1R) on nearby presynaptic inhibitory terminals, which can induce a long-lasting reduction of presynaptic GABA release probability (*39*–*43*). The eCB receptor, CB1R, and mGluR5 are present in vLGN (fig. S10, A and B) (*45*, *46*), and the majority of plHVA-innervated vLGN neurons highly express the mGluR5 receptor (fig. S10, C to E). We therefore investigated whether eCB-dependent iLTD in vLGN could mediate learned suppression of escape.

We first tested whether learning to suppress fear responses was dependent on activation of mGluR5 by infusing mGluR5 antagonist, MPEP, in vLGN (Fig. 5A). Blocking mGluR5 receptors specifically in vLGN compromised learning: mice showed higher escape probabilities to looming stimuli after the learning protocol compared with vehicle-injected littermates (Fig. 5B). Blocking mGluR5 receptors in the hippocampus (dorsal of vLGN) instead had no effect on learning (fig. S10G). Next, we examined if learning was mediated by eCB signaling. We infused a cocktail of eCBs synthesis inhibitors, LEI401+DO34, in vLGN (Fig. 5A). This intervention prevented animals from learning, as they still showed a high probability to escape from looming stimuli after the learning protocol (Fig. 5B). The same effect could be achieved by infusing a CB1 receptor antagonist (rimonabant) in vLGN (Fig. 5B). Inversely, infusion of an CB1 receptor agonist in vLGN caused long-term cessation of escapes to looming stimulus without the learning protocol, demonstrating that eCB signaling in vLGN can drive the suppression of instinctive fear response (fig. S10H). Notably, infusion of the eCB synthesis antagonist into vLGN did not affect escape probabilities to looming stimuli of varying threat levels (using different contrast levels) before learning, showing that blocking of eCB signaling in vLGN does not affect instinctive escape responses or general fear levels (fig. S10I).

Although our results so far indicate that eCB-dependent plasticity in vLGN underlies the learning process, it still remains open whether and how synaptic connectivity in vLGN is altered by learning. We thus performed whole-cell recordings in vLGN, specifically from vLGN neurons receiving input from plHVAs (Fig. 5, C to G). Bath application of eCBs decreased the frequency, but not the amplitude of spontaneous inhibitory postsynaptic currents (sIPSCs) recorded from plHVA-innervated vLGN neurons of naïve mice (Fig. 5D), demonstrating eCB-induced suppression of inhibitory input onto these neurons. To identify learning-induced changes in vLGN circuits, we next performed whole-cell recordings in mice that had undergone our learning protocol and learned to suppress escapes. We found that the frequency but not the amplitude of sIPSCs in plHVA-innervated vLGN neurons was significantly decreased after learning (Fig. 5, E to G), and their excitability was increased (fig. S11C). By contrast, vLGN neurons that did not receive input from plHVAs showed no changes over learning (fig. S11). These data indicate that release probability of GABA from presynaptic inhibitory terminals specifically onto vLGN^{plHVA} neurons is decreased during learning through eCB-dependent iLTD (*44*, *47*) (Fig. 5H).

To formalize these findings, we built a simple computational model recapitulating our experimental results by simulating mean-field activity of two inhibitory neuronal populations both receiving sensory input from the retina, with only one population additionally excited by plHVAs and inhibited by the second population with plastic inhibitory weights (fig. S12).

Discussion

In this study, we uncovered a subcortical synaptic plasticity mechanism for learning to suppress instinctive defensive behavior instructed by visual cortical areas. Our findings highlight the critical role of the neocortex, specifically plHVAs, in modulating instinctive fear responses based on experience. This is consistent with previous work showing that top-down projections from sensory cortex can influence instinctive

behaviors and reflexes (*12*, *13*, *22*, *23*) and suggests that one evolutionary advantageous role of neocortical circuits could be to enable more flexible and adaptive behavior through the regulation of brainstem-driven instincts (*6*–*9*).

We found that higher-order visual cortex was essential for learning to suppress instinctive defensive reactions to visual threats. Notably, visual cortex did not prove necessary for executing and sustaining the adaptive behavior once it was learned. This challenges traditional models that attribute learning and behavioral flexibility mainly to plasticity in telencephalic brain regions. Although visual cortex activity may also change over learning, our results show that plasticity in these cortical circuits does not underlie the behavioral changes after learning. Instead, visual cortex activity crucially contributes to inducing experience-dependent plasticity downstream, namely in the vLGN. vLGN neurons driven by plHVAs increase their responses to the visual threat stimulus over learning, and such increased activity in vLGN circuits abolishes fear responses through their inhibitory influence on downstream areas that mediate escapes from visual threat, such as the superior colliculus (*11*, *35*, *36*). The vLGN, and perhaps caudal prethalamic areas more generally (*35*, *37*), can thus link cognitive, neocortical processes with "hard-wired" brainstem-mediated behaviors, providing a plastic inhibitory control pathway for experience-dependent adaptive behavior.

Learning to suppress fear responses relied on an eCB-mediated form of inhibitory long-term synaptic plasticity, known as iLTD. This mechanism acts on inhibitory synapses onto vLGN neurons activated by plHVAs, decreasing presynaptic release probability. eCB-dependent iLTD has been demonstrated in multiple brain areas as an heterosynaptic in vitro plasticity mechanism induced through activation of glutamatergic mGluR5 receptors through repeated electrical stimulation in brain slices (*40*–*43*). We found that learning to suppress fear responses in vivo depended on eCB release and eCB receptor CB1 activation specifically in vLGN. mGluR5 receptor activation in vLGN was important for learning, but additional pathways could contribute to triggering eCB release in vLGN (*39*–*43*). Moreover, vLGN neurons receiving input from plHVAs were susceptible to eCB-dependent suppression of inhibition and showed decreased inhibitory input after animals had learned to suppress escape responses. Our study thus provides direct evidence of this plasticity mechanism, eCB-mediated decrease of inhibitory input, occurring in vivo to mediate learning. Although the source of the plastic inhibitory input onto plHVA-driven vLGN neurons remains to be identified, it likely stems at least partly from local inhibitory interneurons: our cross-correlogram analysis suggests that plHVA-driven vLGN neurons are inhibited by

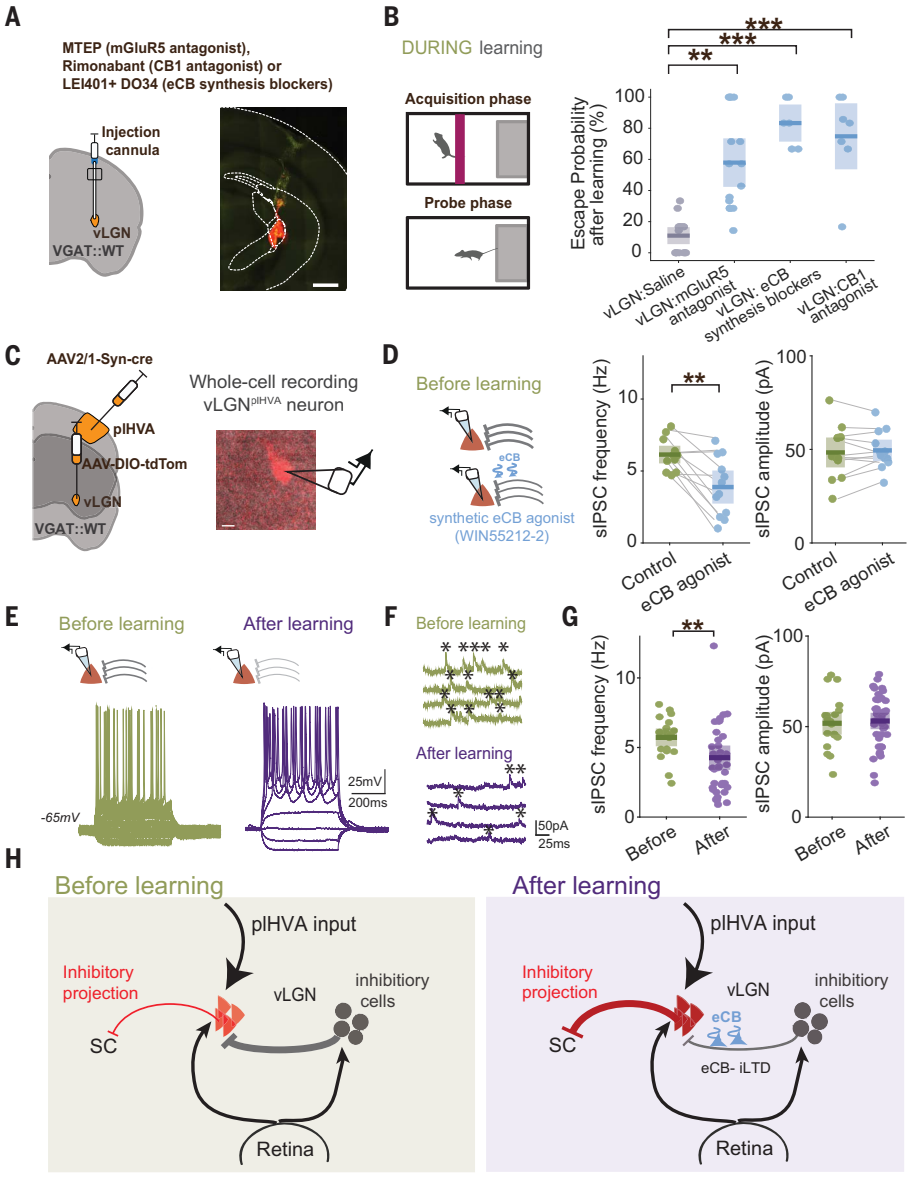

Fig. 5. eCB-mediated long-lasting disinhibition as a mechanism for learning to suppress fear responses. (**A**) (Left) Experimental approach. (Right) Coronal section with an example injection. Scale bar, 1 mm. (**B**) (Left) Schematic of the task design. (Right) Boxplot (with median and interquartile range) of postlearning escape probabilities to 100%-contrast looming stimuli for different reagents injected before the learning protocol; vLGN injection of saline (n = 13 mice), mGluR5 antagonist MTEP (P = 0.001, n = 15 mice), eCB synthesis blockers LEI401 and DO34 (P = 0.0004, n = 6 mice), and CB1 receptor antagonist Rimonabant (P = 0.0008, n = 7 mice). Kruskal-Wallis test followed by Tukey post hoc test was performed for all conditions. Dots indicate individual animals. (**C**) (Left) Experimental approach to visualize vLGN neurons receiving input from plHVAs (vLGN^{plHVA}). (Right) Example image of a recorded vLGN^{plHVA} neuron. Scale bar, 30 μm. (**D**) (Left) Schematic of experiment. (Right) Boxplots of frequency and amplitude of spontaneous inhibitory postsynaptic currents (sIPSCs) in vLGN^{plHVA} neurons recorded with and without bath application of the eCB agonist WIN5521-2 (frequency, P = 0.003; amplitude, P = 0.603; paired t test; n = 12 cells from 4 mice). Dots indicate individual neurons. (**E**) Membrane potential traces of two example vLGN^{plHVA} neurons in response to current injections of different amplitudes before and after learning to suppress escape responses. (**F**) Example traces of sIPSCs under voltage clamp in vLGN^{plHVA} neurons before (green) or after learning (purple). (**G**) Boxplots of frequency and amplitude of sIPSCs recorded from mice before and after learning [frequency, P = 0.002; amplitude, P = 0.827; Kruskal-Wallis test; n = 20 cells from 4 mice (before learning) and 39 cells from 5 mice (after learning)]. Dots indicate individual neurons. (**H**) Schematic of the mechanism underlying learnt suppression of escape responses: eCB-mediated iLTD of presynaptic inhibition onto vLGN^{plHVA} neurons, likely induced through depolarization induced by direct visual looming stimulus input from the retina combined with input from plHVAs. $^{**}P < 0.001$; $^{***}P < 0.001$.

other vLGN neurons before learning but not after learning. Their neural responses to looming stimuli, likely driven by both plHVAs and direct projections from the retina (*34*), thus become released from inhibition during learning and the increased activity of these GABAergic neurons in turn inhibits down-stream target areas to suppress threat-evoked escape reactions (*11*, *35*).

eCBs have long been implicated in the regulation of fear and anxiety and are necessary for extinction of fear conditioning (*48*, *49*). The suppression of instinctive fear responses studied in this work and the extinction of learnt fear share similarities in that both involve active learning to attenuate defensive behaviors in response to a stimulus that no longer predicts danger (*50*). However, these two forms of learning likely engage distinct neural circuits and may differ in their specificity and time course (*49*, *51*). The plasticity mechanism described in this study is likely part of a larger network for regulating defensive behavior, including processes in downstream areas, superior colliculus and periaqueductal gray, as well as complementary top-down pathways through the basal ganglia, hypothalamus, and amygdala (*21*, *51*–*56*).

The ability to suppress instinctive fear responses when threat expectations are violated is an ethologically crucial form of behavioral adaptation, the absence of which could lead to inappropriate or excessive fear responses (*56*). Such maladaptive fear processing is a hallmark of fear and anxiety disorders and posttraumatic stress disorder (*52*, *57*). Dysfunction of pathways through vLGN [also called pregeniculate nucleus in primates (*58*)] or impairments in eCB-dependent plasticity could thus contribute to these disorders. Conversely, targeting these pathways, for example, by using deep brain stimulation, or enhancing eCB-dependent plasticity within these circuits may facilitate suppression of maladaptive fear responses, suggesting new therapeutic strategies for fear-related disorders.

REFERENCES AND NOTES

1. N. Tinbergen, *The Study of Instinct* (Oxford Univ. Press, 1951).
2. D. Mobbs, P. C. Trimmer, D. T. Blumstein, P. Dayan, *Nat. Rev. Neurosci.* **19**, 419–427 (2018).
3. D. A. Evans *et al.*, *Nature* **558**, 590–594 (2018).
4. T. Branco, P. Redgrave, *Annu. Rev. Neurosci.* **43**, 417–439 (2020).
5. D. Rossier, V. La Franca, T. Salemi, S. Natale, C. T. Gross, *Proc. Natl. Acad. Sci. U.S.A.* **118**, e2013411118 (2021).
6. W. H. R. Rivers, *Instinct and the unconscious: A contribution to a biological theory of the psycho-neuroses* (Cambridge Univ. Press, ed. 2, 2006), pp. 66–70.
7. D. A. Evans, A. V. Stempel, R. Vale, T. Branco, *Trends Cogn. Sci.* **23**, 334–348 (2019).
8. S. Sangha, M. M. Diehl, H. C. Bergstrom, M. R. Drew, *Neurosci. Biobehav. Rev.* **108**, 218–230 (2020).
9. C. H. Rankin *et al.*, *Neurobiol. Learn. Mem.* **92**, 135–138 (2009).
10. S. C. Lenzi *et al.*, *Curr. Biol.* **32**, 2972–2979.e3 (2022).
11. A. Fratzl *et al.*, *Neuron* **109**, 3810–3822.e9 (2021).
12. S. Natale, M. Esteban Masferrer, S. Deivasigamani, C. T. Gross, *Eur. J. Neurosci.* **54**, 6044–6059 (2021).
13. T. B. Franklin *et al.*, *Nat. Neurosci.* **20**, 260–270 (2017).
14. A. Tafreshiha, S. A. van der Burg, K. Smits, L. A. Blömer, J. A. Heimel, *J. Exp. Biol.* **224**, jeb230433 (2021).
15. M. Yilmaz, M. Meister, *Curr. Biol.* **23**, 2011–2015 (2013).
16. G. De Franceschi, T. Vivattanasarn, A. B. Saleem, S. G. Solomon, *Curr. Biol.* **26**, 2150–2154 (2016).
17. C. Shang *et al.*, *Nat. Commun.* **9**, 1232 (2018).
18. A. S. Bittencourt, E. M. Nakamura-Palacios, H. Mauad, S. Tufik, L. C. Schenberg, *Neuroscience* **133**, 873–892 (2005).
19. J. T. DesJardin *et al.*, *J. Neurosci.* **33**, 150–155 (2013).
20. P. Tovote *et al.*, *Nature* **534**, 206–212 (2016).
21. K. Wu *et al.*, *Neuron* **111**, 3650–3667.e6 (2023).
22. B. H. Liu, A. D. Huberman, M. Scanziani, *Nature* **538**, 383–387 (2016).
23. X. R. Xiong *et al.*, *Nat. Commun.* **6**, 7224 (2015).
24. J. Liu, Y. He, A. Lavoie, G. Bouvier, B.-H. Liu, *Nat. Commun.* **14**, 8467 (2023).
25. L. L. Glickfeld, S. R. Olsen, *Annu. Rev. Vis. Sci.* **3**, 251–273 (2017).
26. M. Jin, L. L. Glickfeld, *Curr. Biol.* **30**, 4682–4692.e7 (2020).
27. M. L. Andermann, A. M. Kerlin, D. K. Roumis, L. L. Glickfeld, R. C. Reid, *Neuron* **72**, 1025–1039 (2011).
28. C. Stringer, M. Michaelos, D. Tsyboulski, S. E. Lindo, M. Pachitariu, *Cell* **184**, 2767–2778.e15 (2021).
29. P. M. Goltstein, S. Reinert, T. Bonhoeffer, M. Hübener, *Nat. Neurosci.* **24**, 1441–1451 (2021).
30. S. Ruediger, M. Scanziani, *eLife* **9**, 1–24 (2020).
31. L. Tang, M. J. Higley, *Neuron* **105**, 346–354.e5 (2020).
32. N. D. Nguyen *et al.*, *Nature* **625**, 110–118 (2024).
33. V. J. Estela-Pro, R. D. Burwell, *Behav. Neurosci.* **136**, 101–113 (2022).
34. U. Sabbagh *et al.*, *J. Neurochem.* **159**, 479–497 (2021).
35. A. Fratzl, S. B. Hofer, *Neuron* **110**, 2728–2742 (2022).
36. L. D. Salay, A. D. Huberman, *Cell Rep.* **37**, 109792 (2021).
37. X. Wang, *Trends Neurosci.* **43**, 82–87 (2020).
38. Z. V. Guo *et al.*, *Neuron* **81**, 179–194 (2014).
39. G. L. Gerdeman, J. Ronesi, D. M. Lovinger, *Nat. Neurosci.* **5**, 446–451 (2002).
40. V. Chevaleyre, P. E. Castillo, *Neuron* **38**, 461–472 (2003).
41. B. D. Heifets, P. E. Castillo, *Annu. Rev. Physiol.* **71**, 283–306 (2009).
42. A. Bilbao *et al.*, *iScience* **23**, 100951 (2020).
43. Y. W. Wu *et al.*, *Cell Rep.* **10**, 75–87 (2015).
44. J. Xu, Y. Zhu, A. Contractor, S. F. Heinemann, *J. Neurosci.* **29**, 3676–3684 (2009).
45. S. M. Sunkin *et al.*, *Nucleic Acids Res.* **41** (D1), D996–D1008 (2013).
46. G. Govindaiah, C. L. Cox, *J. Neurophysiol.* **101**, 1761–1773 (2009).
47. C. Lüscher, K. M. Huber, *Neuron* **65**, 445–459 (2010).
48. B. Lutz, G. Marsicano, R. Maldonado, C. J. Hillard, *Nat. Rev. Neurosci.* **16**, 705–718 (2015).
49. G. Marsicano *et al.*, *Nature* **418**, 530–534 (2002).
50. K. M. Myers, M. Davis, *Mol. Psychiatry* **12**, 120–150 (2007).
51. B. A. Silva, C. T. Gross, J. Gräff, *Learn. Mem.* **23**, 544–555 (2016).
52. P. Tovote, J. P. Fadok, A. Lüthi, *Nat. Rev. Neurosci.* **16**, 317–331 (2015).
53. A. V. Stempel *et al.*, *Curr. Biol.* **34**, 3031–3039.e7 (2024).
54. J. P. Fadok *et al.*, *Nature* **542**, 96–100 (2017).
55. W. Menegas, K. Akiti, R. Amo, N. Uchida, M. Watabe-Uchida, *Nat. Neurosci.* **21**, 1421–1430 (2018).
56. C. T. Gross, N. S. Canteras, *Nat. Rev. Neurosci.* **13**, 651–658 (2012).
57. J. E. Sherin, C. B. Nemeroff, *Dialogues Clin. Neurosci.* **13**, 263–278 (2011).
58. K. Niimi, T. Kanaseki, T. Takimoto, *J. Comp. Neurol.* **121**, 313–323 (1963).
59. S. Medoros, Overwriting an instinct: visual cortex instructs learning to suppress fear responses, Zenodo (2024); https://zenodo.org/uploads/14249472.

ACKNOWLEDGMENTS

We thank M. Lohse, A. Fratzl, and M. Valero for their feedback on the manuscript; Mrsic-Flogel and Hofer Lab members for helpful discussions; and A. Fratzl for initial discussions, conceptualization, and help with experimental setups and analysis. We thank S. C. Lenzi and T. W. Margrie for help with the behavioral paradigm. We thank M. Li for animal husbandry and genotyping; Neurogears (A. Almeida, J. J. Frazão, and G. Lopes) for help building the behavioral setup; A. M. Koltchev and L. Daveau for help with animal handling; R. Campbell for help with serial two-photon imaging; J. Broni-Trabi for help with RNAscope; and P. Nowak from the Sainsbury Wellcome Centre viral core for providing viruses. We thank SWC FabLabs for technical support and A. Covelo for advice on endocannabinoid experiments. **Funding:** This work was supported by the Sainsbury Wellcome Centre core grant from the Gatsby Charitable Foundation and the Wellcome Foundation (090843/F/09/Z), a Wellcome Investigator Award (S.B.H., 219561/Z/19/Z), an EMBO postdoctoral fellowship (S.M., EMBO ALTF 327-2021), and a Wellcome Early Career Award (S.M., 225708/Z/22/Z). **Author contributions:** Conceptualization: S.M. and S.B.H.; Methodology: S.M., S.B.H., and N.V.; Investigation: S.M., P.B., and N.V.; Experimental setup: S.M. and P.B.; Computational model conceptualization: C.C., S.M., and S.B.H.; Computational model investigation: C.C.; Funding acquisition: S.M. and S.B.H.; Writing – original draft: S.M. and S.B.H.; Writing – review & editing: S.M., S.B.H., P.B., N.V., and C.C. **Competing interests:** The authors declare that they have no competing interests. **Data and materials availability:** Data have been made available and deposited in Zenodo (*59*). **License information:** Copyright © 2025 the authors, some rights reserved; exclusive licensee American Association for the Advancement of Science. No claim to original US government works. https://www.science.org/about/science-licenses-journal-article-reuse. This research was funded in whole or in part by the Wellcome Foundation (090843/F/09/Z, 219561/Z/19/Z, and 225708/Z/22/Z), a cOAlition S organization. The author will make the Author Accepted Manuscript (AAM) version available under a CC BY public copyright license.

SUPPLEMENTARY MATERIALS

science.org/doi/10.1126/science.adr2247
Materials and Methods
Figs. S1 to S12
References (*60*–*74*)
MDAR Reproducibility Checklist

Submitted 17 July 2024; accepted 6 January 2025
10.1126/science.adr2247